Single and Multi-Objective Approaches to 3D Evolutionary Aerodynamic Design Optimization

Martina Hasenjäger, Toyotaka Sonoda, Bernhard Sendhoff, Toshiyuki Arima

2005

Preprint:

This is an accepted article published in Sixth World Congress on Structural and Multidisciplinary Optimization ({WCSMO6}). The final authenticated version is available online at: https://doi.org/[DOI not available]

6^{th} World Congress on Structural and Multidisciplinary Optimization
Rio de Janeiro, 30 May - 03 June 2005, Brazil

Single and Multi-Objective Approaches to 3D Evolutionary Aerodynamic Design Optimization

Martina Hasenjäger

Honda Research Institute Europe GmbH
Offenbach/Main, Germany
martina.hasenjaeger@honda-ri.de

Toyotaka Sonoda

Wako Nishi R&D Center, Honda R&D Ltd.
Wako-shi, Japan
toyotaka_sonoda@n.n.rd.honda.co.jp

Bernhard Sendhoff

Honda Research Institute Europe GmbH
Offenbach/Main, Germany
bs@honda-ri.de

Toshiyuki Arima

Wako Research Center, Honda R&D Ltd.
Wako-shi, Japan
toshiyuki_arima@n.w.rd.honda.co.jp

1. Abstract
In this paper, we present the application of evolutionary optimization techniques to the three dimensional aerodynamic design optimization of a gas turbine stator blade. This problem is characterized on the one hand by a high dimensional search space, which results from the need to build a 3D model of the blade, and on the other hand by an extremely expensive data acquisition process, namely the analysis of the 3D flow around the blade. We use a compact, yet flexible B-spline surface model that is optimized using an evolutionary strategy with covariance matrix adaptation (ES-CMA), an algorithm that decouples the population size from the problem dimension and hence needs only small populations and relatively few fitness function evaluations. Although aerodynamic design optimization often is treated as a single objective optimization problem by minimizing solely the aerodynamic loss, the problem is inherently multi-objective. We consider as a second objective the variation of the circumferential static pressure distribution and compare several methods to incorporate this second objective into the optimization: (i) using simple linear aggregation of the two objectives, (ii) rendering the second objective as constraint, and (iii) using multi-objective optimization techniques to determine the Pareto front. We discuss advantages and drawbacks of these methods in terms of their feasibility for our optimization task and hence, more generally, for tasks that are characterized by extremely high costs of data acquisition, e.g. where the evaluation of the objective function for optimization is computationally demanding and time consuming.
2. Keywords: aerodynamic design optimization, evolutionary strategies, covariance matrix adaptation, multi-objective optimization, real world application

3. Introduction
We present the application of evolutionary optimization techniques to the 3D aerodynamic design optimization of an ultra-low-aspect-ratio (ULAR) gas turbine stator blade. This kind of stator blades is only rarely used in gas turbines because of their relatively poor stage efficiency as compared to the more conventional high-aspect-ratio (HAR) turbines. The reason for this presumably lies in the complex 3D nature of the flow in the ULAR case and the complex interaction of the secondary flow with the transonic main flow. With respect to design optimization this has two consequences: on the one hand the advanced design principles developed for HAR blades cannot be exploited to improve the efficiency of the ULAR turbine stator blades because the flow characteristics in both cases are too different. On the other hand we cannot resort to relatively fast two dimensional or quasi three dimensional methods for flow analysis but have to analyze the full three dimensional flow, a computationally expensive task.
From the optimization point of view 3D aerodynamic design optimization constitutes an interesting problem for several reasons. The need to build a 3D model of the design inevitably renders the problem high dimensional. The exploration of a high-dimensional search space, however, requires a large number of data points. In the worst case the number of necessary data points scales exponentially with the search dimension [1]. In 3D aerodynamic design optimization this constitutes a serious problem because here acquisition of a data point means simulation of the fluid dynamic properties of the design under consideration. Computational analysis of 3D flows is still a challenging task. Even with high performance parallel codes this still may take hours. So the ultimate goals in approaching such a kind of problem must be to restrict the problem dimension and to choose methods that are able to cope with sparse data.
Another crucial question in every optimization problem is the formulation of the objective function. In aerodynamic design optimization, traditionally the minimization of the aerodynamic loss, i.e. the average pressure loss, is chosen as optimization target. However, we must not forget that this is an extreme simplification of the problem. In fact, the pressure loss is only one among many quantities that an engineer takes into account when assessing the blade performance. That means, design optimization, like most real world applications, is inherently a multi-objective optimization problem. In this paper, we consider and discuss four approaches to design optimization that span the whole range from single objective optimization via reformulating the multi-objective problem as a single objective problem to real multi-objective optimization. As a first guess we use the single objective of minimizing the mass-averaged total pressure loss. While this yields satisfactory results, we found that it is desirable to include a second objective, the minimization of the variation of the circumferential static pressure distribution. This renders the problem multi-objective. As a first approach we address this multi-objective optimization problem in the simplest way, namely by linear aggregation of the two objectives. The drawback here

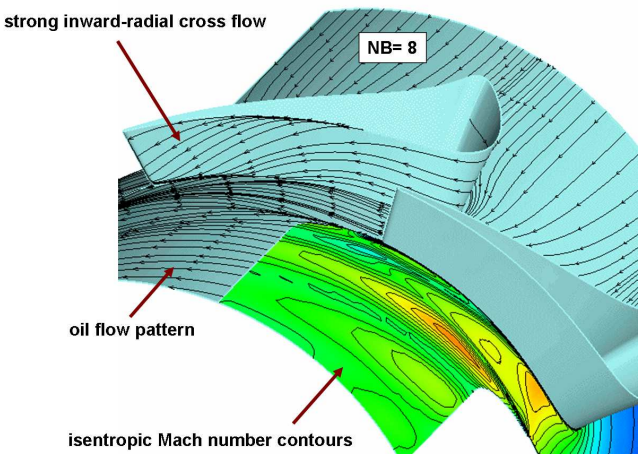

Figure 1: Ultra low aspect ratio turbine stator blades and their flow fields. The blade count is NB=8.

is – besides the linearity of the combination – the ad-hoc choice of the relative weights. Indeed as our results show, the static pressure variation has received too much attention during the optimization.
There are two principle ways to approach this problem and from which a better balance of the two criteria can be expected. First, we render the second criterion as constraint thus avoiding the additional complications induced by multi-objective optimization. Second, we avoid the combination of both objectives and use multi-objective optimization to determine the Pareto front.
In the next section, we introduce the optimization task and present our optimization framework. In Sect. 5, we discuss single objective and multi objective approaches to the solution of this problem. The results from this problem are presented in Sect. 6. Finally in Sect. 7, we will discuss advantages and drawbacks of these methods in terms of their feasibility for our optimization task and hence, more generally, for tasks that are characterized by extremely high costs of data acquisition, e.g. where the evaluation of the objective function for optimization is computationally demanding and time consuming.

4. Three Dimensional Turbine Blade Design Optimization

The aerodynamic design that we optimize is part of a gas turbine that is used in small business jets. In particular, we focus on the turbine part of the engine which is composed of several rows of airfoil cascades. Some of these rows, the rotors, are connected to the central shaft of the engine and rotate at high speed thus driving the engine's fan and compressor and converting gas energy to mechanical energy. The other rows, the stators, are fixed and serve to keep the flow from spiraling around the axis. Our goal is to optimize the design of the turbine stator blades.

4.1. The Turbine Stator Blade

In our case, the stator is of a special type. It is a so-called ultra-low-aspect-ratio (ULAR) stator that is made up of only 8 stator blades. This is a very small number compared to 20 - 60 blades that are used in more conventional turbine designs. For details on the design specifications of the ULAR stator refer to [2].
ULAR stator blades have rarely been adopted as turbine components because of their relatively poor performance. From the flow field based on CFD calculations that is shown in Fig. 1 it can be seen that there is a very strong inward-radial cross flow on the blade suction side and – due to the interaction of the secondary flow with the transonic main flow – the flow field near the hub-end-wall is very complicated. Consequently, the loss near the hub region is considerably increased as compared to conventional HAR blades. We can assume that the higher loss near the hub region leads to poor stage efficiency. Indeed, the stage efficiency is experimentally demonstrated to be only about 88% [2]; a value which is below the efficiency reached by state of the art HAR turbines that reach values well above 90%.
Nevertheless, there are considerable benefits when adopting low aspect ratio blades. For example, for a low number of stator blades rotor blade resonance, and hence material fatigue, is considerably reduced.
The above mentioned ULAR blade flow characteristics make it unlikely that the advanced design principles developed for conventional high aspect ratio blades will help to improve the efficiency of ULAR stator blades: The flow phenomena that can be observed are too different to enable direct exploitation of design principles developed for high aspect ratio blades. Hence ULAR stator blades are excellent candidates for numerical optimization. The goal of optimization from the engineering point of view is not only to increase blade efficiency, i.e. ultimately to reduce the engine's fuel consumption, but also to identify new design concepts that control the strong secondary flow, or in other words, the three-dimensional nature of the flow.
The main performance index that characterizes a turbine blade is the pressure loss. However, there are other quantities that have to be taken into account. The most important of these is in our case the variation of the static outlet pressure. As already mentioned above, axial flow turbine components in a gas turbine engine are in general comprised of a row of stator blades followed by a row of rotor blades. The stator blades are located just upstream of the rotor blades and generate shock waves in a transonic turbine stage. This means the downstream rotor blades are surrounded by a highly distorted static pressure field. It is well known that the aerodynamic performance of the downstream rotor significantly deteriorates due to this distorted pressure field. Therefore, it is important that

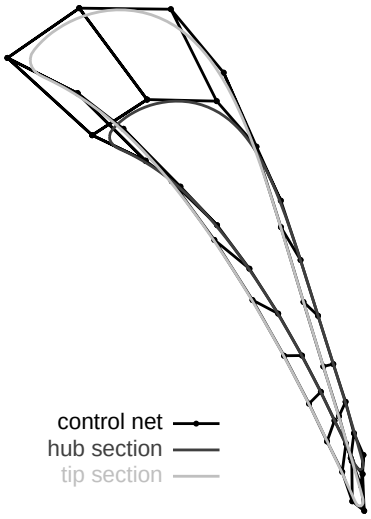

Figure 2: The blade model is created from the hub section (dark gray) and the tip section (light gray) of the baseline blade. These sections are defi ned by 25 control points each. The control net of the baseline surface model, that connects neighboring control points is depicted by a black line.

considerations in blade design not only include the loss reduction of the upstream stator but also the homogeneity of the static pressure field downstream of the stator since this will result in a performance increase of the downstream rotor. Besides this aerodynamic reason for including the static outlet pressure in the design process there is also a mechanical reason. As already mentioned, in transonic turbine stages the exit static pressure field of the stator is highly non-uniform in the pitchwise direction. The rotor periodically traverses this non-uniform field and is exposed to large static pressure fluctuations and consequently to large variations of aerodynamic forces. This contributes to high cycle fatigue and may result in unexpected blade failure.

4.2. Evolutionary Algorithms

Evolutionary algorithms [3] are a class of stochastic optimization algorithms whose use in design optimization problems is well established by now [4]. In our approach to 3D turbine blade optimization we use a special variant of evolutionary algorithms, namely an evolution strategy (ES) with covariance matrix adaptation (CMA) [5]. The basic idea of CMA-ES is to make maximum use of the information contained in the search history for self-adaptation of the search direction which is defined in terms of the covariance matrix of a normal distribution from which new tentative solutions or, in the language of evolutionary algorithms, new individuals are drawn. Thereby the population size in the evolutionary strategy is decoupled from the dimension of the search space. This means that a drawback of stochastic search, the need for evaluation of a large number of possible solutions, is alleviated.
Especially the latter feature is indispensable in 3D blade optimization which is characterized by a fundamental conflict: on the one hand we need a 3D parametric model of the design which entails a high-dimensional design space. As a consequence a large number of different designs has to be evaluated during optimization. On the other hand each evaluation of the blade performance is a computationally extremely demanding task so that only a limited number of evaluations can be afforded.

4.3. Blade Model

A crucial point in design optimization is the parametric model of the geometry that will be optimized since this determines the design space. There are a number of requirements on the design of a proper blade model. Among these are

- flexibility: the model must be flexible enough to allow for a wide variety of different designs,
- compactness: the number of parameters describing the model must be low enough to allow for reasonable convergence times of the optimization algorithm, and
- locality: variations of a single model parameter should result in only local variations of the model and should not affect the global model shape.

A good choice to fulfill these requirements is to use non-uniform rational B-spline (NURBS) surfaces [6] to represent the blade. A B-spline surface is a tensor product of two B-spline curves and hence is defined by two parameters, a set of control points and two knot vectors, one for each parameter. Usually not all of these parameters are subject to optimization. Often the variables in the design optimization problem are given by the coordinates of the control points only. However, the suitable number of control points must be chosen with care: the use of too few control points may unnecessarily restrict the design space and exclude potentially interesting designs while the use of too many control points complicates the optimization problem and additionally may have unwanted side-effects like the creation of cusps or even self-intersections of the resulting surfaces.
Due to manufacturing reasons, our blade geometry is defined by two sections, the hub section and the tip section. The remaining blade geometry is defined by linear interpolation between these two sections. The blade model consists of a B-spline surface defined by a

periodically closed cubic B-spline in one parameter direction and a second order open B-spline in the other direction. The hub section and the tip section of the blade are each modeled using 25 control points so that all in all 50 control points are used. The control net of the blade model and the section geometries are shown in Fig. 2.
Using the coordinates of the 50 three-dimensional control points directly as design variables would result in a 150-dimensional search space. Fortunately, we can exploit two facts to reduce the search space dimension to only 88. We use closed periodic splines in the first parameter direction of the blade surface model to achieve a closed and seamless shape that has no beginning or end points. This implies that the first d and the last d control points of each blade section coincide. Here d denotes the degree of the splines which is $d = 3$ in our case of cubic splines. This means that each of the two blade sections is defined by only $25 - 3 = 22$ independent control points. The periodic control points need not be taken into account as design variables so that in total we only have to consider 44 control points. Furthermore we can exploit the fact that the hub section as well as the tip section of the blade are defined to lie on cylindrical surfaces. This means the z-coordinates of the control points are implicitly fixed by the blade geometry. Hence we only need to consider the x- and y-coordinates of the non-periodic control points as design variables and so we are left with only $2 \times 44 = 88$ design parameters.

4.4. Flow Analysis

For the evaluation of a blade design, an analysis of the aerodynamic properties of the proposed design is necessary. Eventually the design will be built and tested in a wind tunnel. This procedure would be too expensive and time consuming during the design process, so the usual approach is to simulate the flow and thus to estimate the dynamic properties of the blade designs.
For these simulations we used the parallelized 3D Navier-Stokes flow solver HSTAR3D [7], with Wilcox's k-ω two equations model [8]. In order to obtain a high resolution of the boundary layer development, CFD calculations for the baseline blade have been performed prior to optimizations for determining the grid size. The computational grid for the solution of the Navier Stokes equation consisted of $175 \times 52 \times 64 = 582,400$ cells. For each evaluated blade design a new grid was generated. This is a relatively inexpensive operation that takes on average about 40 seconds on an AMD Opteron 2 GHz double processor. The flow analysis, however, is an extremely time consuming task that takes between 2 hours and 3.5 hours on 4 AMD Opteron 2 GHz double processor machines depending on the number of flow solver iterations needed for convergence. So the calculation of about 300 generations comprised of 10 individuals of the evolutionary optimization, takes about 6 weeks time using a cluster of 40 computers!

5. Single and Multi-Objective Approaches

A complex optimization problem like aerodynamic design optimization is inherently multi-objective even if often only a single objective is taken into account for optimization. But also if multiple objectives are employed, the problem often is rendered as a single objective one and solved with familiar and efficient single objective optimization methods. An example for this approach is to aggregate multiple objectives linearly weighted by an appropriate choice of parameters and to solve the resulting single objective problem. As long as the choice of the parameters is well founded, this approach is indeed very sensible since it is the computationally most efficient one.
Another approach that is often used to avoid more complicated and less efficient multi-objective approaches is to use all but one objective as soft constraints, i.e. small deviations from the target are tolerated. Such an approach is especially appropriate where it is desirable but not mandatory to minimize the objectives used as constraints while an increase of the objective value above a certain value is not tolerable.
Multi-objective optimization has been the subject of intense research in the recent years in the field of evolutionary computation [9]. In contrast to single objective optimization, which aims at finding a single optimal solution, multi-objective optimization strives for searching a set of optimal solutions in problems with possibly conflicting objectives. This Pareto set is characterized by the fact that no solution from this set is better than another Pareto solution in all objectives involved. Since evolutionary algorithms inherently operate on sets, i.e. a population of solutions, they seem to be particularly suitable for multi-objective optimization problems. The drawback here is that most multi-objective optimization algorithms seem to require more function evaluations than efficient single-objective methods like the derandomized evolution strategies with cumulative step-size adaptation. As already mentioned, the larger number of required function evaluations poses a problem when each function evaluation is computationally demanding, like for aerodynamic design optimization problems [10, 11], other fluid-dynamic problems [12] or even multi-disciplinary problems [13]. In these cases, effort has been undertaken to minimize the needed population size [11] or to employ meta-models [14, 15]. Since we deal with a particularly computationally demanding aerodynamic optimization problem in this paper, we have to employ algorithms which minimize the required number of individual evaluations. We use both "standard" static aggregated methods and the dynamic weight aggregation method [16, 17] which employs an evolution strategy to represent the set of Pareto optimal solutions in an archive.

5.1. Fitness Functions and Constraints

The main performance index in aerodynamic blade design is the aerodynamic loss of the blade which is measured by the mass averaged pressure loss ω. The use of this quantity as performance measure is certainly a coarse but viable simplification of the problem. In practice, a number of other quantities play an important role in the assessment of the blade quality. Unfortunately, it often is difficult to detail the crucial factors and anticipate the influence of a combination of these quantities on the optimization.
We identified the variation of the pitch-wise static outlet pressure $\mathrm{PST}_{\mathrm{VAR}}$ as a second quantity that should be controlled explicitly in the optimization in order to reduce the stator-rotor-interaction in the turbine. This quantity is defined by

$$\mathrm{PST}_{\mathrm{VAR}} = \max_{\mathrm{i=1\ldots K}} \left(\left| \max_{\mathrm{j=1\ldots L}} \{\mathrm{PST(i,j)}\} - \min_{\mathrm{j=1\ldots L}} \{\mathrm{PST(i,j)}\} \right| \right) , \tag{1}$$

where i is the span-wise and j the pitch-wise index in the computational grid that was used in the flow analysis.

In addition to these two objectives, we used a number of geometrical and manufacturing constraints that were included in the objective function as penalty terms. These were (i) the outflow angle β_2 and (ii) the mass flow rate $\dot{m}$ which are determined as a result of the flow analysis. The outflow angle was constrained to lie in a range of $\delta\beta_2$ around the design value $\beta_{2,\mathrm{design}}$. In the same way, the mass flow rate was constrained to lie in a range of $\delta\dot{m}$ around the design value $\dot{m}_{\mathrm{design}}$. The other constraints concern the blade geometry and basically can be considered as manufacturing constraints. These are (ii) the minimum blade thickness Θ_{min} that was constrained to be bigger than the design value $\Theta_{\mathrm{min,design}}$, (iii) the minimum trailing edge thickness Θ_{min} that had to be at least $\Theta_{\mathrm{TE,min}}$, and (iv) the blade solidity s_{max} that was constrained from above by $s_{\mathrm{max,design}}$. The constraints were included in the objective function in form of a weighted sum c

$$c = \sum_{i=1}^{5} w_i\, t_i^2 \qquad \text{with} \qquad \begin{array}{l} t_1{=}\max(0, |\beta_{2,\mathrm{design}} - \beta_2| - \delta\beta_2) \\ t_2{=}\max(0, |\dot{m}_{\mathrm{design}} - \dot{m}| - \delta\dot{m}) \\ t_3{=}\max(0, \Theta_{\mathrm{min,design}} - \Theta_{\mathrm{min}}) \\ t_4{=}\max(0, \Theta_{\mathrm{TE,min,design}} - \Theta_{\mathrm{TE,min}}) \\ t_5{=}\max(0, s_{\mathrm{max}} - s_{\mathrm{max,design}}) \end{array} \tag{2}$$

The blade model that was used to initialize the optimization lies within the feasible region of the design space. According to Eq. (2) only violated constraints contribute to the objective function. The weights $w_i, i = 1 \ldots 5$ on the constraints were chosen such that the contribution of a violated constraint by far outweighs the contribution of the objectives in order to quickly drive the search back into the feasible region.
We conducted a series of both single and multi-objective optimizations using the following objective functions and optimization approaches, respectively:

A. We only minimized the pressure loss and observed $\mathrm{PST}_{\mathrm{VAR}}$. This is a single objective approach with the objective function

$$f_1 = \omega + c \rightarrow \min, \tag{3}$$

where c are the constraints according to Eq. (2).

B. We used simple linear aggregation of the two objectives according to

$$f_2 = w_{01}\omega + w_{02}\mathrm{PST}_{\mathrm{VAR}} + \mathrm{c} \rightarrow \min, \tag{4}$$

Here the weights w_{01} and w_{02} of both objectives are constant throughout the optimization and were initially chosen such that both objectives contributed equally to the objective function. Again c denotes the constraints defined in Eq. (2). This approach constitutes a simple, naïve approach to multi-objective optimization.

C. We minimized the pressure loss and included the static outlet pressure as a constraint thus turning the multi-objective problem into a single objective one. Thus the objective is

$$f_3 = \omega + w_0\, [\min(0, \mathrm{PST}_{\mathrm{VAR,init}} - \mathrm{PST}_{\mathrm{VAR}})]^2 + \mathrm{c} \rightarrow \min, \tag{5}$$

where $\mathrm{PST}_{\mathrm{VAR,init}}$ is the initial blade's value of $\mathrm{PST}_{\mathrm{VAR}}$ and w_0 is the corresponding weight. The constraints c are included according to Eq. (2).

D. We used the true multi-objective approach of dynamic weight aggregation (DWA) [16, 17]. In this algorithm the two objectives are linearly aggregated according to

$$f_4(t) = w_{01}(t)\ \ \omega + w_{02}(t)\ \mathrm{PST}_{\mathrm{VAR}} + \mathrm{c} \rightarrow \min, \tag{6}$$

Here the weights of the two objectives are varied dynamically, gradually, and periodically during the optimization according to $w_{01}(t) = \left|\sin\left(\frac{2\pi}{p}t\right)\right|$ and $w_{02}(t) = 1 - w_{01}(t)$, where p defines the period of the variation and t is given by the generation of the population. This approach can easily be combined with arbitrary evolutionary strategies which has the advantage that we can retain using CMA-ES and the associated small populations. The constraints again are included according to Eq. (2).

6. Results

In our experiments, we used a (μ, λ) CMA-ES with parameter settings as described in [5]. We used $\mu = 1$ parent individual and $\lambda = 10$ offspring individuals. The strategy parameters σ were initialized with $\sigma = 0.1$. This value gave good results in preliminary tests with a wider range of possible initialization values. We did not use recombination. The simulations were run on a cluster of AMD Opteron 2GHz double processors. The optimization results that we present in this work, are not the converged solutions of the evolution strategy but snapshots taken after about 1 to 2 months of simulation time. Indeed it is difficult to estimate both convergence and expected future progress. However, one can use several heuristics to stop the optimization process, among those are small diversity in the solutions during recent generations, sufficient improvement reached, and allocated computation time exceeded.
We ran 4 single- and multi-objective variants of the optimization as detailed in Sect. 5.1 above, cf. Eq. (3) - Eq. (6). In the multi-objective optimization using DWA according to Eq. (6) we used a period $p = 100$ generations, i.e. the weights w_{01} and w_{02} were periodically varied from 0 to 1 within 50 generations. The results reported for this run were taken after 426 generations.
A detailed analysis from the aerodynamic point of view of the optimized blade with objective function Eq. (3) is given in [18]. In this paper we will restrict our discussion of the results to a comparison of the various optimization approaches.

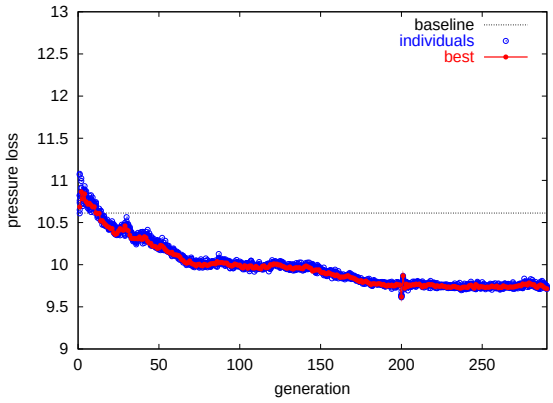

(a) pressure loss

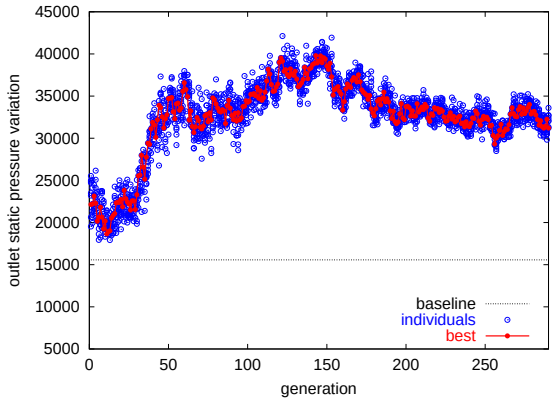

(b) variation in static outlet pressure

Figure 3: The developing of (a) the pressure loss and (b) the variation of the static outlet pressure in the case of single objective optimization according to Eq. 3. The single individuals are marked by open circles, the fi tness-best individuals of each generation are connected. The baseline blade performance is indicated by a dotted line.

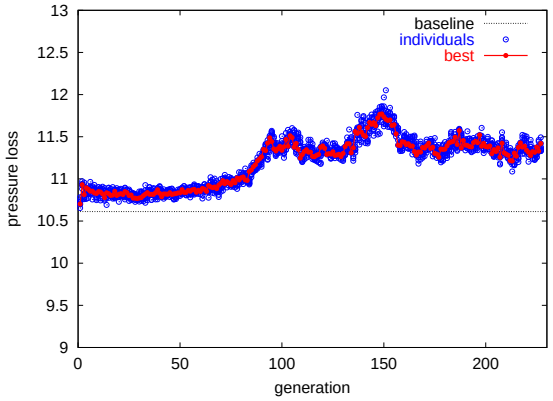

(a) pressure loss

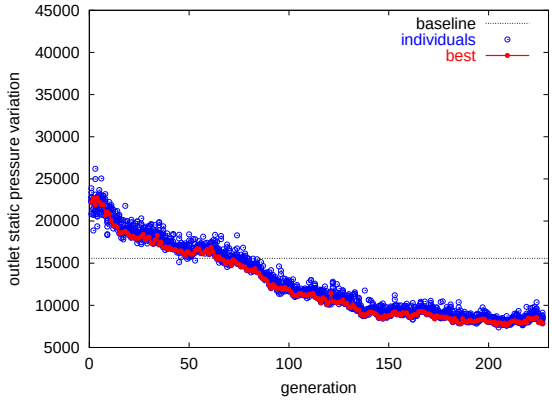

(b) variation in static outlet pressure

Figure 4: The developing of (a) the pressure loss and (b) the variation of the static outlet pressure in the case of linear aggregation of the objectives according to Eq. 4. The single individuals are marked by open circles, the fi tness-best individuals of each generation are connected. The baseline blade performance is indicated by a dotted line.

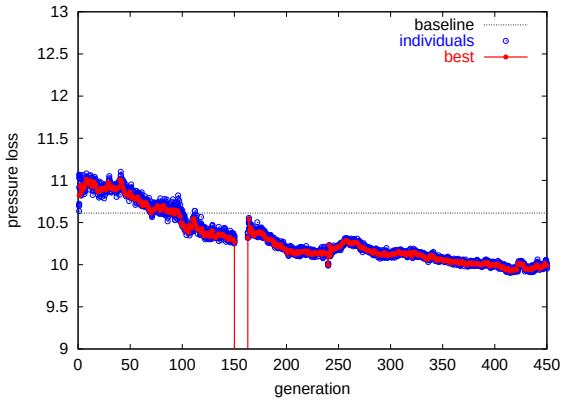

(a) pressure loss

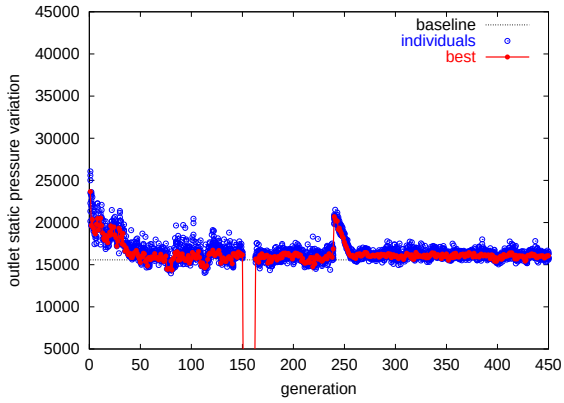

(b) variation in static outlet pressure

Figure 5: The developing of (a) the pressure loss and (b) the variation of the static outlet pressure in the case of single objective optimization of the pressure loss subject to a soft constraint on the static outlet pressure according to Eq. 5. The single individuals are marked by open circles, the fi tness-best individuals of each generation are connected. The baseline blade performance is indicated by a dotted line.

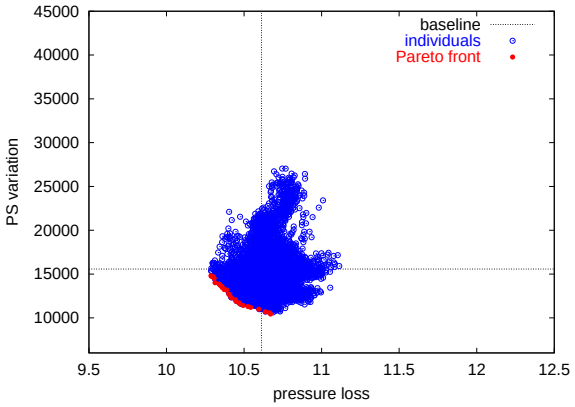

Figure 6: The Pareto front from the multi-objective optimization with DWA according to Eq. 6. The individuals that build the Pareto front are marked by filled circles.

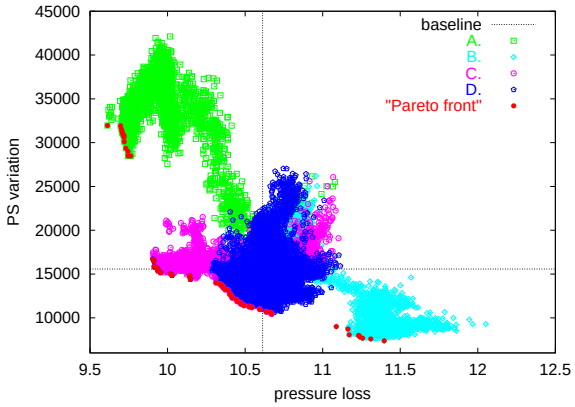

Figure 7: The "Pareto front" aggregated from all four optimization runs. Here "baseline" denotes the performance of the baseline blade. A - minimization of the pressure loss, cf. Eq. 3, B - static linear aggregation of the two objectives, cf. Eq. 4, C - minimization of the pressure loss subject to an upper bound on the static outlet pressure, cf. Eq. 5, D - multi-objective optimization using dynamic weight aggregation, cf. Eq. 6. The individuals that build the Pareto front are marked by filled circles.

In Figs 3 to 5 we show the evolution of the two criteria that we considered in this study. Figs 3 (a) and (b) show the pressure loss and the variation of the static outlet pressure, respectively, as a function of the number of generations in the single objective optimization case given by Eq. 3. From the optimization point of view this simulation was quite successful: a reduction in the pressure loss of about 10% was achieved. However, as shown in Fig. 3 (b), this was reached at the expense of a considerable increase in the variation of the static pressure which is a very undesirable behavior from the engineering point of view for reasons explained in Sec. 4.1.

This increase was the reason why we included $\mathrm{PST}_{\mathrm{VAR}}$ explicitly in the objective function. The results of doing so by static linear weight aggregation according to Eq. 4 are shown in Fig. 4. As a first approach in this case, we chose the weights of the two objectives such that initially both objectives received the same weight. Fig. 4 (a) and (b) show that this choice is not the best one. The variation of the static outlet pressure received too much weight, so that the optimizer was able to reduce only $\mathrm{PST}_{\mathrm{VAR}}$ while allowing an increase of the pressure loss of about 9%.

In a second approach, we included the variation of the static outlet pressure as a soft constraint according to Eq. 5. We bounded $\mathrm{PST}_{\mathrm{VAR}}$ from above using approximately the value of the initial blade. The results are shown in Figs 5 (a) and (b). The constraint is effective in controlling $\mathrm{PST}_{\mathrm{VAR}}$ while at the same time the pressure loss is reduced. Compared with Fig. 3 (a) this reduction is achieved at a slightly slower pace. The vertical lines in Fig. 5 indicate that from generation 150 to generation 160 the process of grid generation and flow analysis failed for the whole population. In principle, this is critical because it may lead to a failure of the whole optimization process. But here the optimizer was sufficiently robust to tolerate the missing results from the flow analysis and to drive the population back to a region in which flow analysis was possible with relatively small loss in performance.

The results from the multi-objective optimization using dynamic weight aggregation according the Eq. 6 are shown in Fig. 6 (a). Here we plotted for each individual that was produced in the optimization process the values of $\mathrm{PST}_{\mathrm{VAR}}$ against the value of the pressure loss achieved. The Pareto optimal individuals are marked by filled circles. An individual i^* is Pareto optimal if all other individuals i have a higher value for at least one of the criteria or else have the same value for all criteria. In Fig. 6 also the performance of the initial blade design is plotted as a dotted line for each of the two objectives. This means all blade designs in the upper right quadrant are inferior to the initial blade and all blade designs in the lower left quadrant are superior to the initial blade with respect to both objectives. From Fig. 6 (a) we see that using multi-objective optimization techniques it is possible to reduce $\mathrm{PST}_{\mathrm{VAR}}$ and the pressure loss at the same time. However, the progress in this case is much slower than in the single objective optimization.

In Fig. 7 we summarized the results from all four optimizations, plotted them in the same way as the results in Fig. 6 and again marked the Pareto points of the complete data by filled circles. This representation allows us to directly compare the results from all optimizations with respect to the two involved optimization criteria and at the same time we gain a more complete impression of the Pareto front in this problem. The designs found by solely minimizing the pressure loss – denoted by A. in Fig. 7 – clearly achieve the lowest pressure loss of all designs but are also characterized by the highest static pressure variation. The other extreme, a high pressure loss and a low variation in the outlet pressure, is represented by the solutions from the static linear aggregation of both objectives – denoted by B. in Fig. 7. This is due to the minor influence of the pressure loss in this case that was caused by the choice of the weights in the linear aggregation Eq. (4). Best at simultaneously minimizing both objectives is the multi-objective approach using dynamic weight aggregation – denoted by D. in Fig. 7, while using $\mathrm{PST}_{\mathrm{VAR}}$ as a soft constraint – denoted by C. in Fig. 7 – yields solutions with low pressure loss and slightly decreased static pressure variation.

7. Conclusion

Three dimensional aerodynamic design optimization constitutes a challenging problem because the need to work with a 3D model of the design entails a high dimensional search space and in general requires large amounts of data. These data, however, are obtained by analyzing the 3D flow around the blade, a process that consumes huge amounts of computation time which makes data acquisition expensive. This is the main limiting factor in the optimization problem. Hence decisions on the choice of models and algorithms must

be governed by the goals of using a compact, yet flexible computational model and optimization algorithms that are able to cope with sparse data in order to allow for only a small number of objective function evaluations in the optimization. Our proposal here is to use a B-spline model of the blade and to optimize this using a derandomized evolution strategy with cumulative step-size adaptation, namely the covariance matrix adaptation [5]. This algorithm effectively decouples the population size from the dimension of the search space thus facilitating the use of small populations and hence relatively few data points.

The target in this study was to identify new aerodynamic designs that achieve low aerodynamic losses and low pressure variations. The trade-off relation between both objectives has been previously pointed out in the literature [19]. From the optimization point of view the combination of the different criteria and constraints constitutes an interesting problem. In this paper, we employed and compared several methods to combine the two objectives. The simplest way to do so is static linear aggregation. Its main advantage is that the problem remains single objective and more efficient algorithms can be used than are available for multi-objective optimization. The drawbacks, besides the linearity of the combination, are the ad-hoc choice of the relative weights and the inflexibility of the weights. A successful application of this method requires careful exploration of the weight space, a possibly time-consuming task that may well outweigh the advantage of being able to use efficient single objective optimization algorithms. To make matters worse, the appropriate weighting of the constraints may change during optimization. Indeed as our results show, the ad-hoc choice of the weights drew too much attention towards the static pressure variation. In other words, the selection pressure towards smaller pressure loss values was not sufficient.

We pursued two principle ways to proceed. First, we regarded the static pressure variation as a constraint. Thus, we set the variation of the static outlet pressure of the baseline blade as a soft constraint, so that slight overshooting was penalized only slightly, and only optimized the pressure loss. This again was a single objective optimization approach with the aforementioned advantages that will yield good results if, as in our case, it is sufficient to impose a bound on all but one of the objectives.

Secondly, we used a multi-objective approach, dynamic weight aggregation [16, 17] which searches for the Pareto front by dynamically, gradually, and periodically changing the weighting factors of a linear aggregation of the objectives during optimization. The advantage of this approach is that it can easily be combined with arbitrary evolutionary strategies, so that we can retain using CMA-ES and the associated small populations. This is especially important in cases like ours where a large number of individuals cannot be afforded because of hardware and time restrictions. Small populations would not be possible with all multi-objective evolutionary algorithms. NSGA-II [20], for example, a successful and popular method that is based on genetic algorithms or real coded genetic algorithms requires substantially larger populations than CMA-ES.

8. References

1. R. Bellman. *Adaptive Control Processes: A guided Tour*. Princeton University Press, New Jersey, 1961.
2. N. Kuno and T. Sonoda. Flow characteristics in a transonic ultra-low-aspect-ratio axial turbine vane. *Journal of Propulsion and Power*, 20(4):596–603, 2004.
3. T. Bäck, D. B. Fogel, and T. Michalewicz, editors. *Evolutionary Computation 1: Basic Algorithms and Operators*. Institute of Physics, 2000.
4. A. Osyczka. *Evolutionary Algorithms For Single And Multicriteria Design Optmization*. Physica-Verlag, 2002.
5. N. Hansen and A. Ostermeier. Completely derandomized self-adaptation in evolution strategies. *Evolutionary Computation*, 9(2):159–195, 2001.
6. G. Farin. *Curves and Surfaces for Computer-Aided Geometric Design*. Academic Press, San Diego, 4 edition, 1997.
7. T. Arima, T. Sonoda, M. Shirotori, A. Tamura, and K. Kikuchi. A numerical investigation of transonic axial compressor rotor flow using a low-Reynolds-number $k - \epsilon$ turbulence model. *ASME Journal of Turbomachinery*, 121:44–58, 1999.
8. D. C. Wilcox. Reassessment of the scale-determining equation for advanced turbulence models. *AIAA Journal*, 26:1299–1310, 1988.
9. K. Deb. *Multi-Objective Optimization Using Evolutionary Algorithms*. Wiley, 2002.
10. S. Obayashi, Y. Yamaguchi, and T. Nakamura. Multiobjective genetic algorithm for multidisciplinary design of transonic wing planform. *Journal of Aircraft*, 34(5):690–693, 1997.
11. B. Naujoks, W. Haase, J. Ziegenhirt, and T. Bäck. Multi-objective airfoil design using single parent population. In *Proceedings of the Genetic and Evolutionary Computation Conference*, pages 1156–1163. Morgan Kaufmann, 2002.
12. T. Okabe, K. Foli, M. Olhofer, Y. Jin, and B. Sendhoff. Comparative studies on micro heat exchanger optimization. In *Congress on Evolutionary Computation (CEC)*, volume 1, pages 647–654. IEEE Press, 2003.
13. K. Chiba, S. Obayashi, K. Nakahashi, and H. Morino. High-fidelity multidisciplinary design optimization of wing shape for regional jet aircraft. In *Evolutionary Multi-criterion Optimization*, pages 621–635. Springer Verlag, 2005.
14. Z. Z. Zhou, Y. S. Ong, P. B. Nair, A. J. Keane, and K. Y. Lum. Combining global and local surrogate models to accelerate evolutionary optimization. *IEEE Transactions On Systems, Man and Cybernetics - Part C*, 2005.
15. Y. Jin, M. Olhofer, and B. Sendhoff. A framework for evolutionary optimization with approximate fitness functions. *IEEE Transactions on Evolutionary Computation*, 6(5):481–494, 2002.
16. Y. Jin, M. Olhofer, and B. Sendhoff. Dynamic weighted aggregation for evolutionary multi-objective optimization: Why does it work and how? In *Proceedings of the Genetic and Evolutionary Computation Conference GECCO*, pages 1042–1049, 2001.
17. Y. Jin, T. Okabe, and B. Sendhoff. Solving three objective optimization problems using evolutionary dynamic weighted aggregation: Results and analysis. In *Proceedings of the Genetic and Evolutionary Computation Conference - GECCO*, pages 636–637, 2003.
18. M. Hasenjäger, B. Sendhoff, T. Sonoda, and T. Arima. Three dimensional aerodynamic optimization for an ultra-low aspect ratio transonic turbine stator blade. ASME Paper GT2005-68680, 2005.

19. M. L. Shelton, B. A. Gregory, S. H. Lamson, H. L. Moses, R. L. Doughty, and T. Kiss. Optimization of a transonic turbine airfoil using artificial intelligence, CFD and cascade testing. ASME Paper 93-GT-161, 1993.
20. K. Deb, A. Pratap, S. Agarwal, and T. Meyarivan. A fast and elitist multiobjective genetic algorithm: NSGA-II. *IEEE Transactions on Evolutionary Computation*, 6(2), 2002.